Article

Modeling of Continuous Slug Flow Cooling Crystallization towards Pharmaceutical Applications

Anne Cathrine Kufner, Michael Rix, and Kerstin Wohlgemuth *

Tables and Figures

Table S1. Experimental measured and calculated slug length. Experimental data taken from [1,2]. Calculated slug length for the initial fit [3] and the fit conducted in this publication are given. The five parameters $c_1 - c_5$ needed in **Equation 10** are given in **Table 2**.

Q_{tot} / mL min^{-1}	ε_L / -	w_{solid} / g_{solid} g_{sol}^{-1}	$L_{slug,exp}$ / mm	$L_{slug,calc}$ / mm	$L_{slug,fit}$ / mm
20.02	0.338	1.322	7.58	9.12	6.96
60.76	0.323	1.430	4.94	7.63	5.25
19.46	0.684	1.490	15.16	17.09	15.39
60.84	0.654	1.460	10.64	13.40	10.71
18.63	0.350	6.030	7.14	9.34	7.30
60.07	0.331	5.522	5.59	7.72	5.36
19.64	0.668	5.329	15.12	16.37	14.74
59.02	0.672	5.237	14.89	14.12	11.55
19.68	0.332	2.029	7.19	9.07	6.94
59.17	0.336	1.908	4.75	7.78	5.37
20.14	0.656	2.255	15.29	15.82	13.99
59.66	0.668	1.782	10.18	13.96	11.27
19.91	0.333	5.686	6.96	9.06	7.01
60.81	0.327	5.831	5.29	7.66	5.29
20.14	0.661	5.465	16.3	16.02	14.40
59.84	0.662	5.831	11.08	13.72	11.08
39.94	0.500	3.685	7.96	10.40	8.00
39.61	0.498	3.193	8.06	10.38	7.97
40.10	0.501	4.424	8.37	10.41	8.02
40.15	0.501	3.588	10.3	10.40	7.98
20.00	0.500	1.000	8.35	11.49	9.43
20.00	0.500	1.000	7.85	11.49	9.43
20.00	0.500	0	7.72	11.50	9.10
19.96	0.501	0	9.77	11.52	9.12
19.94	0.501	0	9.44	11.53	9.13
19.88	0.503	0	9.27	11.56	9.17
20.00	0.500	0	10.09	11.50	9.10
29.92	0.499	0	9.32	10.84	8.26
39.76	0.504	0	8.48	10.50	7.81
59.92	0.500	0	7.27	9.82	7.02

Table S2. Experimental measured and calculated pressure drops. Experimental data taken from [1,2].

Q_{tot} / mL min^{-1}	ε_L / -	w_{solid} / g_{solid} g_{sol}^{-1}	L_{tubing} / m	Δp_{exp} / mbar	Δp_G / mbar	Δp_{PM} / mbar	Δp_{mp} / mbar	Δp_{tot} / mbar
20.02	0.338	1.322	7.50	188.0	0.1	4.6	199.2	203.9
60.76	0.323	1.430	7.50	269.0	0.4	13.7	252.2	266.3
19.46	0.684	1.490	7.50	220.0	0.1	8.7	182.3	191.1
60.84	0.654	1.460	7.50	310.0	.2	27.4	250.6	278.2
18.63	0.350	6.030	7.50	217.5	0.1	5.0	198.8	203.9
60.07	0.331	5.522	7.50	278.0	0.4	14.9	255.7	270.9
19.64	0.668	5.329	7.50	239.0	0.1	9.7	187.5	197.3
59.02	0.672	5.237	7.50	355.0	0.2	30.2	240.7	271.1
19.68	0.332	2.029	7.50	195.5	0.1	4.5	196.6	201.2
59.17	0.336	1.908	7.50	270.0	0.4	13.6	256.6	270.6
20.14	0.656	2.255	7.50	215.5	0.1	9.0	192.9	201.9
59.66	0.668	1.782	7.50	370.0	0.2	27.5	243.5	271.2
19.91	0.333	5.686	7.50	200.0	0.1	5.2	196.6	201.9
60.81	0.327	5.831	7.50	272.5	0.4	14.4	255.9	270.6
20.14	0.661	5.465	7.50	202.2	0.1	10.3	190.0	200.4
59.84	0.662	5.831	7.50	363.5	0.2	28.7	247.6	276.4
39.94	0.500	3.685	7.50	270.0	0.2	14.6	257.6	272.3
39.61	0.498	3.193	7.50	272.0	0.2	14.1	257.4	271.7
40.10	0.501	4.424	7.50	305.0	0.2	14.8	258.0	273.0
40.15	0.501	3.588	7.50	277.5	0.2	14.1	258.9	273.2
19.96	0.501	0	26.05	829.0	0.3	16.5	855.7	872.5
19.94	0.501	0	18.25	540.0	0.2	11.5	599.5	611.2
19.88	0.503	0	15.00	449.5	0.2	9.4	492.4	502.0

Table S3. Operating conditions of a typical SFC setup taken from Termühlen et al. [1,4] for the calculation of the individual effect's influence on gas expansion.

L_{tubing} / m	Q_{tot} / mL min^{-1}	ε_L / -	ϑ_{in} / °C	ϑ_{out} / °C	Δp_{tot} / bar
26.5	20	0.5	50	30	1

Table S4. Comparison of operating conditions and setup of the SFC with the derivation of the correlation by QIAN AND LAWAL [3]. The superficial velocity is the velocity of one phase alone in the tubing.

	Mixer diameter / mm	Mixer type / -	Contact angle / °	Superficial velocity / m s^{-1}
QIAN AND LAWAL [3]	0.25 – 3	T-junction	90 – 110	0.010 – 0.250
This publication	3	T-junction	102	0.014 – 0.083

Table S5. Experimental measured, hydrodynamic and calculated RTs.

Experiment	Q_{tot} / mL min^{-1}	ε_L / -	L_{tubing} / m	Experimental RT / min	Hydrodynamic RT / min	Actual RT / min
[2]	20	0.50	7.50	2.84	2.98	2.83
[2]	40	0.50	7.50	1.45	1.49	1.4
[2]	60	0.50	7.50	0.98	0.99	0.928
[1]	20	0.50	37.00	12.92	14.49	12.28
[1,4]	20	0.33	26.50	8.02	10.52	9.33
[1,4]	20	0.66	26.50	9.32	10.52	10.09
[1,4]	40	0.50	26.50	4.33	5.26	4.63
[1]	20	0.50	7.50	2.70	3.02	2.88

[1]	20	0.50	15.70	5.20	6.23	5.74
[1]	20	0.50	33.75	10.55	13.40	11.60
[1,4]	20	0.50	13.25	4.33	5.26	4.90

Table S6. Comparison of the mean heat transfer resistances for the heat transfer from the bulk TM to the environment for the experiment with a SFC tubing length of L_{tubing} = 7.5 m, PM flow rate of Q_{PM} = 10 ml min^{-1}, and TM volume flow rate of Q_{TM} = 37 ml min^{-1}.

$R_{\text{TM,wall}}$ / K W^{-1}	R_{wall} / K W^{-1}	$R_{\text{wall,ENV}}$ / K W^{-1}	R_{tot} / K W^{-1}
5.5	25.1	305.9	336.5

Table S7. Comparison of the operating conditions for the growth rate constants fitted by HOHMANN ET AL. [5] with the operating conditions investigated in this publication.

	κ / K min^{-1}	ϑ_{in} / °C	ϑ_{out} / °C
Literature growth rate [5]	0.5 - 1.0	30	24
This publication	1.8 – 3.6	50	30

Table S8. Operating conditions of the reviewed crystallization experiments [1,4,6]. The experiment's labels, SFC lengths, flow rates of PM and TM, the liquid hold-up, cooling rate, and in- and outlet temperatures are given.

Experiment	L_{tubing} / m	Q_{tot} / mL min^{-1}	ε_L / -	Q_{TM} / mL min^{-1}	κ / K min^{-1}	$\vartheta_{\text{PM,in}}$ / °C	$\vartheta_{\text{PM,out}}$ / °C
CR	26.50	40	0.50	64	3.6	50.0	31.4
EPS	26.50	20	0.50	130	1.8	50.0	31.4
EPS33	26.50	20	0.33	161	1.8	50.0	30.8
EPS66	26.50	20	0.66	121	1.8	50.0	31.2
Qmax	26.50	40	0.50	368	1.8	50.0	40.8
VWZ	13.25	20	0.50	203	1.8	50.0	40.6
CVSF 10	26.50	20	0.50	146	2.0	49.9	30.1
CVSF 20	26.50	40	0.50	105	3.9	50.0	29.5

Table S9. Comparison of the agglomeration degree and mean particle size of the seed and product crystals in the crystallization experiments [1,4,6]. Operating conditions are given in **Table A8**.

Experiment	Seed crystals		Product	
	Agglomeration degree / %	d_{50} / µm	Agglomeration degree / %	d_{50} / µm
CR	76.0	281.6	75.5	478.1
EPS	76.0	281.6	79.2	497.4
EPS33	76.0	281.6	86.3	433.7
EPS66	76.0	281.6	88.9	514.9
Qmax	76.0	281.6	78.1	390.1
VWZ	57.7	261.8	85.2	462.4
CVSF 10	61.8	215.3	75.0	448.7
CVSF 20	61.8	215.3	73.9	410.0

Figure S1. Images of seed crystals used (left) and product crystals obtained (right) during crystallization process inside the SFC and taken via dynamic image analysis (QICPIC, Sympatec). No abrasion of the particles is detectable.

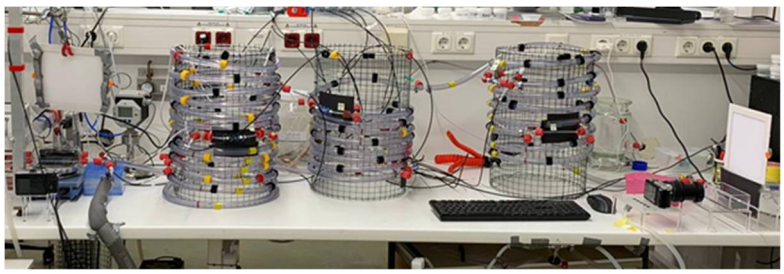

Figure S2. Picture of the experimental SFC setup (growth zone) of the reviewed experiments. The slugs are transported through the coiled tubing and crystallization takes place. Image analysis can be performed after slug formation and at the SFC outlet.

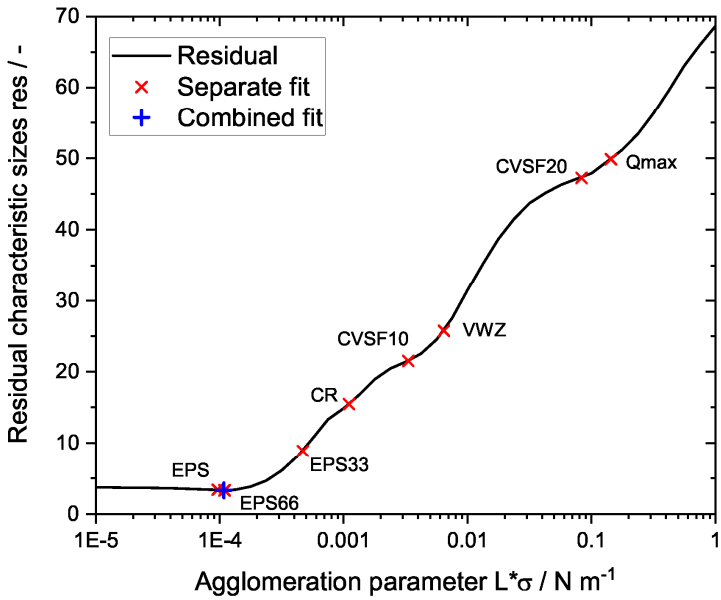

Figure S3. Course of the residual of the PSDs of all experiments combined against the agglomeration parameter (black line). The red crosses depict the residuals of all experiments for the individual fits of each experiment, the blue cross the residual for the combined fit of all experiments together.

Derivations and Equations

Modeling Slug Flow Hydrodynamics

$$Q_{\mathrm{G},1} = Q_{\mathrm{G},0} \cdot \frac{p_0 T_1}{p_1 T_0} \xleftrightarrow{convert\ to\ velocity} v_1 = \frac{Q_{\mathrm{tot}}}{A_{\mathrm{SFC}}} = \frac{Q_{\mathrm{G}}}{A_{\mathrm{SFC}}} + \frac{Q_{\mathrm{PM}}}{A_{\mathrm{SFC}}} = \frac{Q_{\mathrm{G},0} \cdot p_0 \cdot T_1}{A_{\mathrm{SFC}} \cdot p_1 \cdot T_0} + \frac{Q_{\mathrm{PM}}}{A_{\mathrm{SFC}}} \text{ with } A_{\mathrm{SFC}} = \frac{\pi}{4} d_{SFC}^2 \tag{S1}$$

Energy Balance

$$\dot{Q}_{\mathrm{conv,i}} = \dot{m}_{\mathrm{TM}} \cdot c_{\mathrm{p,TM,i}} \cdot T_{\mathrm{TM,i}} \tag{S2}$$

$$\begin{aligned} \dot{Q}_{\mathrm{UC,TM}} &= \varepsilon_{\mathrm{L}} \cdot \dot{Q}_{\mathrm{PM,TM}} + (1-\varepsilon_{\mathrm{L}}) \cdot \dot{Q}_{\mathrm{G,TM}} \\ &= \varepsilon_{\mathrm{L}} \cdot k_{\mathrm{PM,TM}}{}^{*} \cdot A_{\mathrm{UC,TM}} \cdot \left(T_{\mathrm{PM}} - T_{\mathrm{TM,i}}\right) + (1-\varepsilon_{\mathrm{L}}) \cdot k_{\mathrm{G,TM}} \cdot A_{\mathrm{UC,TM}} \cdot \left(T_{\mathrm{G}} - T_{\mathrm{TM,i}}\right) \end{aligned} \tag{S3}$$

* The heat transfer coefficient is calculated following the approach of MUZYCHKA ET AL. [7]

$$\dot{Q}_{\mathrm{TM,ENV}} = k_{\mathrm{TM,ENV}} \cdot A_{\mathrm{TM,ENV}} \cdot \left(T_{\mathrm{TM,i}} - T_{\mathrm{ENV}}\right) \tag{S4}$$

$$\dot{Q}_{\mathrm{i}} = \dot{m}_{\mathrm{i}} \cdot c_{\mathrm{p,i}}(T) \cdot \left(T_{\mathrm{i,in}} - T_{\mathrm{i,out}}\right) \tag{S5}$$

$$\dot{Q}_{\mathrm{c}} = \dot{m}_{\mathrm{c}} \cdot \Delta h_{\mathrm{SL}} \tag{S6}$$

$$\dot{Q}_{\mathrm{EVP}} = \dot{m}_{\mathrm{EVP}} \cdot \Delta h_{\mathrm{SL}} \tag{S7}$$

$$\dot{Q}_{\mathrm{PM,TM}} = \int_0^{L_{slug}} k_{\mathrm{PM,TM}} \cdot \pi \cdot d_{\mathrm{SFC}} \cdot \left(T_{\mathrm{PM}} - T_{\mathrm{TM}}(x)\right) dx \tag{S8}$$

$$\dot{Q}_{\mathrm{PM,TM}} = \pi \cdot d_{\mathrm{SFC}} \cdot \sum_{i=1}^{n} k_{\mathrm{PM,TM}} \cdot \left(T_{\mathrm{PM}} - T_{\mathrm{TM,i}}\right) \cdot \Delta x \tag{S9}$$

$$\frac{\partial T_{\mathrm{PM}}}{\partial t} = \frac{\dot{Q}_{\mathrm{c}} - m_{\mathrm{PM}} \cdot T_{\mathrm{PM}} \cdot \left(c_{\mathrm{p,c}} - c_{\mathrm{p,PM}}(T)\right) \cdot \frac{\partial w_{\mathrm{c}}}{\partial t} - \dot{Q}_{\mathrm{PM,TM}}}{m_{\mathrm{PM}} \cdot \left(T_{\mathrm{PM}} \cdot w_{\mathrm{c}} \cdot \frac{\partial c_{\mathrm{p,c}}}{\partial T_{\mathrm{PM}}} + w_{\mathrm{c}} \cdot c_{\mathrm{p,c}} + (1-w_{\mathrm{c}}) \cdot T_{\mathrm{PM}} \cdot \frac{\partial c_{\mathrm{p,PM}}(T)}{\partial T_{\mathrm{PM}}} + (1-w_{\mathrm{c}}) \cdot c_{\mathrm{p,PM}}\right)} \tag{S10}$$

$$\frac{\partial v}{\partial z} = v_{\mathrm{G},0} \cdot \frac{p_0}{T_0} \cdot \left(\frac{1}{p} \cdot \frac{\partial T}{\partial z} - \frac{T}{p^2} \cdot \frac{\partial p}{\partial z}\right) \tag{S11}$$

Modeling Agglomeration

Calculation of the birth and death rate for a continuous PSD by agglomeration. Birth rate is calculated for a particle of size λ with a particle of size $(L^3 - \lambda^3)^{1/3}$ resulting in a particle of size L. Death rate is calculated for one particle of size L with a particle of arbitrary size λ.

$$B_{\mathrm{Agg}}(L) = L^2/2 \cdot \int_0^L \frac{\beta\left((L^3-\lambda^3)^{1/3}, \lambda\right) \cdot n\left((L^3-\lambda^3)^{1/3}\right) \cdot n(\lambda)}{(L^3-\lambda^3)^{2/3}} d\lambda \tag{S12}$$

$$D_{\mathrm{Agg}}(L) = n(L) \cdot \int_0^{\infty} \beta(L,\lambda) n(\lambda) d\lambda \tag{S13}$$

$$h_{\mathrm{susp}} = 2\chi_{50,\mathrm{V}} \cdot d_{\mathrm{SFC}} \tag{S14}$$

$$L_{\mathrm{susp}} = 2\chi_{50,\mathrm{H}} \cdot L_{\mathrm{slug}} \tag{S15}$$

$$A_{\mathrm{susp}} = (d_{\mathrm{SFC}}/2)^2 \cdot arccos\left(1 - \frac{h_{\mathrm{susp}}}{d_{\mathrm{SFC}}/2}\right) - \left(d_{\mathrm{SFC}}/2 - h_{\mathrm{susp}}\right) \cdot \sqrt{2 d_{\mathrm{SFC}} \cdot h_{\mathrm{susp}} - h_{\mathrm{susp}}^2} \tag{S16}$$

Sensitivity Analysis

Description of the factors $k_{c,1}$ and $k_{c,2}$ in the calculation of the solubility curve:

$$c^*_{\mathrm{Ala}} = 0.11238 \cdot \exp(9.0849 \cdot 10^{-3} \cdot \vartheta^*) = k_{c,1} \cdot \exp\left(k_{c,2} \cdot 10^{-3} \cdot \vartheta^*\right) \tag{S17}$$

Description of the factors $k_{\mathrm{Agg},1}$ and $k_{\mathrm{Agg},2}$ in the agglomeration correlation:

$$L^* \sigma_\gamma = 0.085 \cdot \left(\frac{V_{\mathrm{susp}}}{V_{\mathrm{slug}}}\right)^{1.731} = k_{\mathrm{Agg},1} \cdot \left(\frac{V_{\mathrm{susp}}}{V_{\mathrm{slug}}}\right)^{k_{\mathrm{Agg},2}} \tag{S18}$$

References

[1] M. Termühlen, From design to operation of a continuous slug flow crystallizer for cooling crystallization, Verlag Dr. Hut, München, 2022.

[2] A.C. Kufner, N. Westkämper, H. Bettin, K. Wohlgemuth, Prediction of Particle Suspension State for Various Particle Shapes Used in Slug Flow Crystallization, ChemEngineering 7 (2023) 34. https://doi.org/10.3390/chemengineering7020034.

[3] D. Qian, A. Lawal, Numerical study on gas and liquid slugs for Taylor flow in a T-junction microchannel, Chemical Engineering Science 61 (2006) 7609–7625. https://doi.org/10.1016/j.ces.2006.08.073.

[4] M. Termühlen, M.M. Etmanski, I. Kryschewski, A.C. Kufner, G. Schembecker, K. Wohlgemuth, Continuous slug flow crystallization: Impact of design and operating parameters on product quality, Chemical Engineering Research and Design 170 (2021) 290–303. https://doi.org/10.1016/j.cherd.2021.04.006.

[5] L. Hohmann, T. Greinert, O. Mierka, S. Turek, G. Schembecker, E. Bayraktar, K. Wohlgemuth, N. Kockmann, Analysis of Crystal Size Dispersion Effects in a Continuous Coiled Tubular Crystallizer: Experiments and Modeling, Crystal Growth & Design 18 (2018) 1459–1473. https://doi.org/10.1021/acs.cgd.7b01383.

[6] C. Steenweg, A.C. Kufner, J. Habicht, K. Wohlgemuth, Towards Continuous Primary Manufacturing Processes—Particle Design through Combined Crystallization and Particle Isolation, Processes 9 (2021) 2187. https://doi.org/10.3390/pr9122187.

[7] Y.S. Muzychka, E.J. Walsh, P. Walsh, Heat Transfer Enhancement Using Laminar Gas-Liquid Segmented Plug Flows, Journal of Heat Transfer 133 (2011). https://doi.org/10.1115/1.4002807.